0038-075X/88/1466-0427$02.00/0
SOIL SCIENCE

December 1988
Vol. 146, No. 6
Printed in U.S.A.

DYNAMICS OF PARTIAL ANAEROBIOSIS, DENITRIFICATION, AND WATER IN A SOIL AGGREGATE: SIMULATION

P. A. LEFFELAAR[1]

A simulation model was developed to study the dynamics of partial anaerobiosis and denitrification in unsaturated soil. The model enables one to calculate simultaneously the distribution of water, bacteria, oxygen, carbon dioxide, nitrous oxide, molecular nitrogen, neon, absolute soil atmospheric pressure, nitrate, nitrite, and glucose as a function of space and time in an unsaturated, homogeneous, cylindrical aggregate and the changes in atmospheric composition as a function of time in the chamber that contains the aggregate. Except for water transport, these processes are caused by microbial activity, because roots are not present in the aggregate. The simulation model is the theoretical counterpart of the experimental "soil aggregate system" as studied in a previously described respirometer setup.

The simulated results showed a satisfactory agreement with experimental data: part of the experimental results could be described quantitatively, whereas other data that deviated from the experimental data could be understood by studying the dynamic behavior of the model. Hysteresis in the soil water retention curve resulted in low values of the gas-filled porosities in the outer shell of the partially wetted aggregate, permitting only gaseous exchange through the water phase of soil. As a result anaerobiosis and denitrification occurred.

A major conclusion was that appropriate model parameterization was needed first. To that purpose the model will be used to plan respirometer experiments, to help interpret the experimental data so obtained, and to investigate the relative importance of a number of parameters in a sensitivity analysis. Furthermore, it was concluded that only the interaction of experiment and theory will ultimately lead to a full understanding of the complex soil biological system described.

The objective of this paper is to describe the simulation model, to discuss its parameterization, and to compare some of the simulated results with those of the experimental system described previously.

[1] Dept. of Theoretical Production Ecology, Bornsesteeg 65, 6708 PD Wageningen, The Netherlands.

Received for publication 27 Aug. 1987; revised 5 April 1988.

The release of nitrous oxide and molecular nitrogen by biological denitrification occurs when bacteria capable of denitrification colonize a location where oxygen is absent and water, nitrate, and decomposable organic compounds are present (Delwiche 1981; Ingraham 1981). In aggregated unsaturated soils, anaerobiosis, and hence denitrification, is mainly confined to within the aggregates (Currie 1961; Greenwood 1961). In principle, therefore, denitrification losses from aggregated field soils can be predicted when denitrification losses from individual aggregates and their size distribution are known (Smith 1977, 1980). Denitrification losses from a single aggregate can be predicted successfully only when the spatial distributions of denitrifiers, oxygen, water, nitrate, and decomposable organic compounds can be measured or calculated as a function of time and when these distributions are subsequently combined so that zones of denitrification show up.

Figure 1 depicts some schematic oxygen and water distributions as expected in field aggregates under the assumption of a homogeneous distribution of bacteria and organic compounds and a negligible nitrate production due to nitrification. When oxygen consumption rate does not exceed oxygen supply rate, anoxic conditions will not develop, and equimolar respiration occurs, as indicated by arrows (Fig. 1a). Just after rainfall, mainly the outer shell of an aggregate will be wetted (Leffelaar 1979). The oxygen diffusion rate in the outer shell is then seriously impeded, and when oxygen consumption rate exceeds oxygen supply rate, anoxic conditions arise locally (Fig. 1b). When nitrate from fertilizer has been absorbed with the rainwater, denitrification occurs in the wetted shell. In the center of the aggregate equimolar respiration continues to take place until the oxygen from the enclosed air has been consumed. Then most of the aggregate volume is anaerobic, but deni-

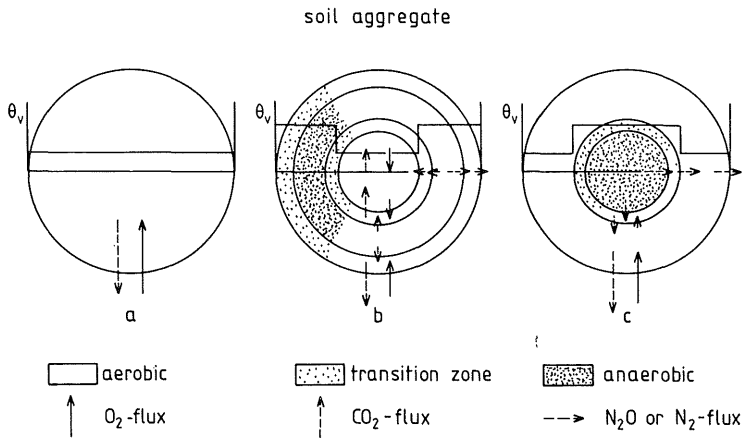

FIG. 1. Schematic of water and oxygen distributions in soil aggregates: a, in a dry period; b, just after a rain shower; c, some time after rainfall. Lengths of arrows indicate relative magnitudes of molar source or sink terms.

trification does not necessarily increase, for the nitrate is mainly concentrated in the wetted shell. The arrows in Fig. 1b indicate a net gas production caused by denitrification. Subsequent redistribution of water may result in a decrease of the anaerobic aggregate volume, and hence of denitrification, when the water content in the wetted soil becomes low enough to get continuous gas-filled pores permitting rapid oxygen diffusion into the aggregate. The distribution of oxygen in Fig. 1c will be found in initially water-saturated aggregates that are drying. Upon further drying their oxygen distributions will adjust to that of Fig. 1a.

These complicated dynamic interactions between biological and physical processes determining denitrification are studied best through the development of a sufficiently detailed explanatory simulation model. Such a model should include a description of microbial activity; movement of gases, water, nitrate, and nitrite; and decomposition of organic compounds in an individual aggregate. The objective of this paper is to describe such an explanatory simulation model, to discuss its parameterization, and to compare the model results with experimental data presented in a previous paper (Leffelaar 1986).

SIMULATION MODEL INTEGRATING SUBMODELS FOR DENITRIFICATION, WATER, SOLUTES, AND GASES

The explanatory simulation model was developed to calculate the distribution of the relevant state variables, here bacteria, water, solutes, and gases, as a function of space and time. As to the geometry, the model refers to an unsaturated cylindrical aggregate in which transport processes are radial. Also the changes in atmospheric composition as a function of time, in the chamber that contains the aggregate, were to be calculated. The cylindrical geometry is a model representation of a soil aggregate from which the upper and lower sides are removed and originates directly from Fig. 1. The simulation model is the theoretical counterpart of an experimental system described previously (Leffelaar 1986). This system consisted of a "macro soil aggregate" with variable water content, placed in a specially designed respirometer. The experimental system was developed at the time to evaluate the present theoretical model; conversely, the theoretical model was developed for full interpretation of the measured data.

The simulation model exposed here comprises four submodels: one for the biological processes of respiration and denitrification, and three for the transport processes of water, solutes (nitrate, nitrite, and decomposable organic compounds, i.e., glucose), and gases (oxygen, carbon dioxide, nitrous oxide, molecular nitrogen, and neon). To calculate the spatial distribution of the various state variables, the system was divided into a number of concentric layers (Frissel and Reiniger 1974; de Wit and van Keulen 1975). The interaction among the four submodels may be demonstrated by the equation of continuity that is solved for each mobile substance in each layer, i.e., Eq. (1)

$$\frac{\partial C_i}{\partial t} = -\frac{\partial J_i}{\partial x} + P_i \qquad (1)$$

All symbols are defined in the appended list of symbols. For instance, the denitrification sub-

model calculates different production rates (P_i) in adjacent aggregate layers, because the bacteria in these layers are subjected to different environmental conditions. Different production rates result in gradients in concentration of substance i. When it concerns a gaseous substance, in principle also gradients in absolute pressure result. The diffusive, dispersive, and mass flow transports that will now occur are contained in the flux (J_i). Integrating Eq. (1) with respect to the time will give the time course of substance i in a layer as a result of the interactions of microbial activity and physical transport processes and the environmental conditions for the bacteria in the layer change. When a substance is inert, e.g., neon, or immobile, e.g., biomass, the production term or the flux term in Eq. (1) equals zero, respectively.

Models remain simplified representations of the real system (de Wit 1982). This, however, does not imply that all models are simple and concise. During the present study it became clear that interactions between submodels, for example, could impose difficulties that are normally not envisaged when such models are developed or used separately. Such interactions, in conjunction with the use of four submodels have resulted in a large, rather complicated computer program (110 pages of code and 120 subroutines) that needed much CPU time (100 min. for a typical run on a VAX-8700 machine). To develop the submodels, numerous assumptions had to be made. A great part of these assumptions has been described elsewhere: the denitrification model by Leffelaar and Wessel (1988); the water-flow model by Dane and Wierenga (1975); and the solute-transport model by Bolt (1979). Therefore, these models are merely summarized below. The gas diffusion model for multinary gas mixtures was also previously discussed (Leffelaar 1987). However, in the integrated model, the interaction of the gases with the water, and with the gas production terms due to respiration and denitrification, complicated the description of the gas-transport model. Therefore, the gas-transport model and the assumptions made for its development will be detailed in this paper.

Respiration and denitrification submodel

The submodel describing respiration and denitrification was discussed in detail in a previous paper (Leffelaar and Wessel 1988). Summarizing, the growth of two groups of heterotrophic strict aerobic bacteria, of which a part is able to denitrify, was calculated by a first-order rate equation. The relative growth rate was described by a double-Monod equation consisting of rate-limiting factors for carbon substrate and oxygen or nitrogenous electron acceptor. Changes in the amounts of glucose carbon, carbon dioxide, oxygen, nitrate, nitrite, nitrous oxide, and molecular nitrogen were described by Pirt's equation, where growth yields and maintenance coefficients of the bacteria are distinguished. The submodel was developed for a homogeneous soil layer. In the simulation model each concentric layer of the aggregate was also assumed homogeneous. Therefore, the denitrification submodel was simply applied in each layer of the aggregate to yield all the production terms P_i in Eq. (1).

Water-transport submodel

Water redistribution in the aggregate was calculated by combining Darcy's law, Eq. (2)

$$J_w = -k \frac{dh}{dx} \tag{2}$$

with the equation of continuity, Eq. (1), where the production term cancelled because roots were absent. Because only horizontal transport of water occurred in the aggregate, gravitational head was omitted in Eq. (2). Both hydraulic conductivity (k) and pressure head of soil water (h) were functions of volumetric water content.

In earlier experiments (Leffelaar 1986, Fig. 4), it appeared that redistribution of water with an initial (schematic) distribution as depicted in Fig. 1b resulted finally in a nonhomogeneous water distribution. This was attributed to the hysteresis phenomenon that may occur in both the water retention curve (Koorevaar et al. 1983) and the hydraulic conductivity-water content curve (Staple 1966; Dane and Wierenga 1975), although others maintain that the latter curve is essentially nonhysteretic (Kool and Parker 1987). Preliminary attempts to model the redistribution process of water in the aggregate without taking hysteresis into account failed: water content was always finally homogeneously distributed. Thus, the submodel for water redistribution had to include hysteresis.

A simulation model describing soil water flow, including hysteresis in the water retention curve and in the hydraulic conductivity-water content

relationship, was reported by Dane (1972)[2] and Dane and Wierenga (1975). Essentially, the scanning curve for wetting (or drying) was forced to converge to the main wetting (or main drying) curve as a function of the difference between the water content at which a reversal of drying to wetting (or wetting to drying) occurred and the actual water content. Dane's model was attractive to use because it combined a reasonable description of the hysteresis phenomenon with an explicit computational scheme similar to that used in the present simulation model. Although other models (e.g., Hopmans and Dane 1986; Kool and Parker 1987) may have a more rigorous theoretical basis than the one of Dane, they have implicit computational schemes that are difficult to adapt to the needs of the present simulation model. The model of Dane and Wierenga (1975) was reformulated so that variable time-step-integration methods could be used to save computer time. Furthermore, the tabular data input of the main drying and main wetting water retention curves and the hydraulic conductivity-water content curves in the model was replaced by equations described by van Genuchten (1980). The parameters in these equations were estimated from the measurements described in the model parameters section below by optimization procedures outlined by van Genuchten (1978).

The water submodel is not affected by the results of other submodels, though in real soil, hydraulic characteristics may be affected by entrapped air and gas pressure (Chahal 1966) resulting from, for example, respiration and denitrification processes; the water submodel, however, directly affects the submodels for the transport processes of solutes and gases.

Solute-transport submodel

Solute transport in the aggregate was calculated by combining Eq. (3)

$$J_s = -D_0\lambda_\omega\theta\frac{dc_s}{dx} - L_d|J_\omega|\frac{dc_s}{dx} + J_w c_s \qquad (3)$$

with the equation of continuity, Eq. (1). The three terms in Eq. (3) represent Fick's first law for diffusive transport, convective dispersion, and convective transport of the solute, respectively. Diffusive flux in soil is reduced compared with that in free water, because the water phase occupies only a fraction of the soil volume (θ), and the diffusion path has a tortuous geometry (λ_w). The product $D_0\times\lambda_w\times\theta$ is often called the effective diffusion coefficient, though it would seem conceptually more appropriate to call $\lambda_w\times\theta$ the flux reduction factor, because the use of D_0 assumes that in the water phase of soil diffusion occurs as in free water. The tortuosity factor, λ_w, was a function of volumetric water content. The convective dispersion coefficient, $L_d\times|J_w|$, is linearly related to the average water flow velocity, $|J_w|$ (Bolt 1979). Concentration of solute (c_s) refers to the water phase of the soil, for no adsorption of solutes to the solid phase was assumed to occur. Numerical dispersion was reduced in the simulation program by computing the convective transport (third term in Eq. (3)) using the linearly interpolated value for c_s at the transition between adjacent compartments (Goudriaan 1973).

Equation (3) was derived and extensively discussed by Bolt (1979) and applied in numerous simulation studies, e.g., de Wit and van Keulen (1975), Frissel and Reiniger (1974), Leistra (1972; 1980), Leistra et al. (1980), and Boesten.[3]

It follows directly from Eq. (3) that the waterflow submodel affects the transport of the solutes as long as the redistribution process continues; diffusive transport, however, will always be present in moist soil, because bacterial activity will hardly ever be similar in adjacent compartments.

Gas-transport submodel

Gas transport in the aggregate was calculated by combining Eq. (4)

$$J_g = -D_{ij}\lambda_g\varepsilon_g\frac{dc_g}{dx} + J_p\frac{c_g}{c} \qquad (4)$$

with the equation of continuity, Eq. (1). The first term in Eq. (4) represents Fick's first law for diffusive transport incorporating area reduction (ε_g) and tortuosity (λ_g), similar to solute

[2] J. H. Dane, 1972, Effect of hysteresis on the prediction of infiltration, redistribution and drainage of water in large soil columns, thesis, New Mexico State Univ., Las Cruces, N. Mex.

[3] J. J. T. I. Boesten, 1986, Behaviour of herbicides in soil: Simulation and experimental assessment, diss., Agric. Univ. Wageningen, p. 263.

transport, but now referring to the gas phase of soil. The binary diffusion coefficients, D_{ij}, were calculated as described previously (Leffelaar 1987) with respect to neon (Ne), because in the experiments nitrogen was replaced by Ne to have the opportunity to measure small quantities of N_2 (Leffelaar 1986). When eventually pressure changes occurred, the binary diffusion coefficients were pressure-corrected. Diffusive transports through the water phase of soil were calculated according to Fick's first law, i.e., the first term in Eq. (4), under the assumption that no coupling of gas fluxes will occur in water. This seems plausible, because the main interactions of dissolved gases will be with the water molecules: water density is very high compared with dissolved gas densities.

The second term is the product of the pressure adjustment flux (J_p) and the relative presence of gas g (c_g/c), that serves to maintain equal total gas pressures on either side of adjacent soil layers. In fact, the second term in Eq. (4) embodies the coupling of fluxes in multinary gas mixtures where water is absent (Leffelaar 1987). The description of diffusion of gases by Eq. (4) in multinary, isothermal, isobaric, ideal-gas mixtures, where in principle differences in total gas pressure were caused solely by unequal binary diffusion coefficients (D_{ij}), agreed to within 10% with results of the rigorous gas kinetic theory for such systems (Leffelaar 1987). The pressure adjustment flux in that case was calculated as the sum of the individual gas fluxes. The integration of the multinary gas diffusion model with the models for water flow and denitrification complicates the calculation of the pressure adjustment flux. This is so, because in a wet soil, where water movement occurs, differences in total gas pressure could also be caused by different gas solubilities in water, mass flow of gas due to water movement, and different source/sink terms in adjacent soil layers, aside from the effect of unequal binary diffusion coefficients. To calculate the pressure adjustment flux in the integrated model, the previously used assumption, that total gas pressure gradients will not occur in adjacent soil layers (Leffelaar 1987), was supplemented with the assumption that partitioning of gases over the water and the gas phase is instantaneous and given by the gas solubility coefficients in water. The details to solve the pressure adjustment flux in the integrated model will be given below. Because pressures and concentrations are interrelated through $c = p/(RT)$, concentrations have been used for convenience in the derivations.

Consider a series of soil layers, as depicted in Fig. 2, that have equal total gas concentrations, $c(l)$, with $l = 1, 2, \ldots, n$. To maintain these mutually similar total gas concentrations, the rate of change of $c(l)$ should be equal in each layer

$$\frac{\Delta c(l)}{\Delta t} = \frac{\Delta c(l+1)}{\Delta t}, \qquad l = 1, 2, \ldots, n \tag{5}$$

with

$$\frac{\Delta c(l)}{\Delta t} = \sum_g \frac{\Delta c'(g, l)}{\Delta t},$$
$$g = 1, 2, \ldots, m, \text{ and } l = 1, 2, \ldots, n \tag{6}$$

The rate of change of concentration of gas g in layer l is defined by the continuity equation written in finite difference form

$$\frac{\Delta c'(g,l)}{\Delta t} = \left(J(g,l) + J_p(l)\frac{\bar{c}(g,l)}{\bar{c}(l)}\right)\frac{A(l)}{V(g,l)} - \left(J(g,l+1) + J_p(l+1) \cdot \frac{\bar{c}(g,l+1)}{\bar{c}(l+1)}\right)\frac{A(l+1)}{V(g,l)} + \frac{S(g,l)}{V(g,l)} \tag{7}$$

where $J(g, l)$ represents Fick's first law, and $V(g, l)$ is the volume that is occupied by gas g in layer l

$$V(g, l) = (\varepsilon_g(l) + K(g)\theta(l))V(l) \tag{8}$$

The assumption of instantaneous partitioning of gas over the gas and water phase is contained in $V(g, l)$. A bar above a symbol indicates the linearly interpolated spatial average of that symbol with respect to the layer in brackets and the previous one. Note that index l may denote the number of the layer or the number of the layer-interface with the previous one. If the water were stationary, Eqs. (5) through (8) would suffice to solve the pressure adjustment flux, as explained below.

Water movement into a layer will induce a countercurrent of gas mixture in its gas phase. Because concentration is amount ($Am(g, l)$) per

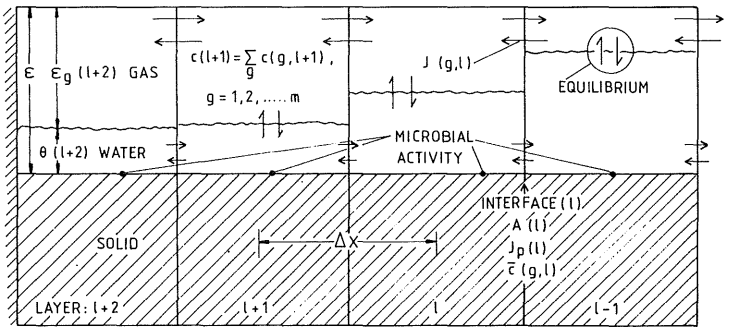

FIG. 2. Geometry of soil system.

unit volume, the rate of change of the concentration of $c(g, l)$ can be written as

$$\frac{\Delta c(g,l)}{\Delta t} = \frac{\Delta}{\Delta t}\left(\frac{Am(g,l)}{V(g,l)}\right) \tag{9}$$

Differentiating the right-hand side of Eq. (9) gives

$$\begin{aligned}\frac{\Delta c(g,l)}{\Delta t} &= \frac{1}{V(g,l)}\frac{\Delta Am(g,l)}{\Delta t} \\ &\quad - \frac{Am(g,l)}{V(g,l)}\frac{1}{V(g,l)}\frac{\Delta V(g,l)}{\Delta t} \\ &= \frac{\Delta c'(g,l)}{\Delta t} - c(g,l)\frac{1}{V(g,l)}\frac{\Delta V(g,l)}{\Delta t}\end{aligned} \tag{10}$$

The term $\Delta c'(g, l)/\Delta t$ of Eq. (10) is defined by Eq. (7); the second term needs further explanation, in particular the rate of change of $V(g, l)$. In Eq. (8), which defines $V(g, l)$, the gas-filled porosity, $\varepsilon_g(l)$, can be eliminated by the identity: $\varepsilon_g(l) = \varepsilon - \theta(l)$. Differentiating the resulting expression yields

$$\frac{\Delta V(g,l)}{\Delta t} = (K(g)-1)V(l)\frac{\Delta\theta(l)}{\Delta t} \tag{11}$$

The last derivative represents the net rate of change of water content, what follows directly from the water-flow submodel: $(J_w(l)A(l) - J_w(l + 1)A(l + 1))/V(l)$. The principal equation for the rate of change of total gas concentration in layer l is obtained by substituting this last expression into Eq. (11), then substituting Eqs. (7) and (11) in Eq. (10), and finally taking the sum over the rates of change of all gases as meant by Eq. (6)

$$\begin{aligned}\frac{\Delta c(l)}{\Delta t} &= \sum_g\left(\frac{A(l)}{V(g,l)}\left(J(g,l) + J_p(l)\frac{\bar{c}(g,l)}{\bar{c}(l)}\right)\right) \\ &\quad - \sum_g\left(\frac{A(l+1)}{V(g,l)}\left(J(g,l+1)\right.\right. \\ &\quad \left.\left. + J_p(l+1)\frac{\bar{c}(g,l+1)}{\bar{c}(l+1)}\right)\right) \\ &\quad + \sum_g\frac{S(g,l)}{V(g,l)} \\ &\quad - \sum_g\left(c(g,l)\left(\frac{(K(g)-1)(J_w(l)A(l) - J_w(l+1)A(l+1))}{V(g,l)}\right)\right)\end{aligned} \tag{12}$$

To take account of the diffusive, dispersive, and mass transports of gases in the water phase of soil, these were summed and added to the terms $J(g, l)$ and $J(g, l + 1)$ as if they formed part of the gas phase fluxes. These transports were calculated by Eq. (3), in which the appropriate constants were substituted.

To solve Eq. (12) for the pressure adjustment fluxes $J_p(l)$, two situations need be distinguished for the present simulation model: (1) all layers have gas-filled porosities exceeding a certain critical value ε_g^{crit}, and exchange of gases between soil and atmosphere takes place via both gas and water phases. ε_g^{crit} is assumed to be the value where air permeability is just measurable (Le Van Phuc and Morel-Seytoux 1972); such layers are further referred to as *gas-continuous layers*; (2) a number of consecutive layers are gas-continuous, but they are sealed from the

atmosphere by one or more layers that have gas-filled porosities smaller than ε_g^{crit}. When the first situation occurs, atmospheric pressure is maintained, and $\Delta c(l)/\Delta t = 0$ for all layers. The set of linear equations needed to solve $J_p(l)$ was obtained as follows: equate Eq. (12) to zero for all layers; rewrite the summation terms to separate the terms containing $J_p(l)$ from other terms; and bring all terms containing $J_p(l)$ to the left of the equals sign. No outflow of gas occurs from the last layer, e.g., the $(l + 2)$ layer in Fig. 2, because it is the center of the cylindrical aggregate, and $J(g, l + 1)$, $J_p(l + 1)$, and $J_w(l + 1)$ in Eq. (12) equal zero. Each equation (except the last) of the set of linear equations now contains terms with $J_p(l)$ and $J_p(l + 1)$, and the set may be written in matrix notation from which the vector of pressure adjustment fluxes can be solved.

When the second situation occurs, in which a number of gas-continuous layers are enclosed by layers that have very small gas-filled porosities, exchange of gases between soil and atmosphere takes place via the water phase (Fig. 1b). When net gas production differs from the gas transport through the water phase, the total gas pressure in the enclosed layers will change, and the difference between the rates of change in consecutive layers must be zero. The set of linear equations needed to solve $J_p(l)$ was obtained similarly to the previous situation with the modification that at first the difference between each pair of adjacent layers was equated to zero: $\Delta c(l)/\Delta t - \Delta c(l + 1)/\Delta t = 0$, for all l.

The J_p-vector was solved for each time step during the simulation using the mathematical libraries of IMSL (IMSL 1982). Subsequently, the pressure adjustment fluxes $J_p(l)$ were used in Eq. (4).

One problem remains to be solved. Suppose that the initial distribution of water in soil is (schematically) given by Fig. 1b. In the outer layers, where $\varepsilon_g < \varepsilon_g^{crit}$, gas exchange takes place via the water phase, and the total gas concentrations in these layers will undoubtedly be different from the enclosed gas-continuous layers. Because water redistributes, layers at the water front will become gas-continuous, and a jump in total gas concentration will appear. Moreover, when the outer layer becomes gas-continuous, such a jump in total gas concentration will occur at the interface of the aggregate and the surroundings. The principle assumption in this study was, however, that no gradients in total gas concentration could occur in soil when $\varepsilon_g > \varepsilon_g^{crit}$. Therefore, such differences in total gas concentration were adjusted instantaneously, the production terms from the denitrification submodel and the gas transport parameters were recalculated, and then the usual calculations, as described above, were continued. The following equations were derived to achieve this adjustment, resulting in equal total gas concentrations in all adjacent gas-continuous soil layers.

Assume that layer $(l - 1)$ (see Fig. 2) has just become gas-continuous, and that it contains a larger total gas concentration with respect to the adjacent layers l, $l + 1$, etc. The amount of gas from layer $(l - 1)$ that will expand into layer l is defined by Eq. (13)

$$\begin{aligned} \Delta Am(l-1) &= \sum_g \Delta Am(g, l-1) \\ &= \sum_g A_p(l) \frac{c(g, l-1)}{c(l-1)} \end{aligned} \tag{13}$$

A_p denotes the amount of gas needed to adjust the pressures in adjacent layers. Because all consecutive layers, i.e., l, $l + 1$, etc., have similar total gas concentrations, a certain amount of gas from layer l will expand into the next layer and so on. The final total gas concentration (i.e., after the adjustments) in, for instance, layer l, is defined by Eq. (14)

$$c(l) = \sum_g \frac{\begin{aligned} &Am(g, l) + A_p(l) \frac{c(g, l-1)}{c(l-1)} \\ &- A_p(l+1) \frac{c(g, l)}{c(l)} \end{aligned}}{V(g, l)} \tag{14}$$

To solve Eq. (14) for the amounts of gas transferred due to pressure adjustment, the difference between each pair of adjacent layers was equated to zero, similar to the case where a number of gas-continuous layers were enclosed by layers that had gas-filled porosities smaller than ε_g^{crit}. The procedure to obtain the set of linear equations from which the vector A_p was solved was similar to the one to solve the pressure adjustment fluxes described above.

When the new gas-continuous layer contained a smaller total gas concentration with respect to adjacent layers, the direction of the adjustment was reversed, and Eq. (14) was formulated slightly differently. All principles remain unchanged, however.

In the case that the outer soil layer became gas-continuous, total gas concentration in the aggregate was adjusted to that of the surroundings, and, because the chamber that contained the experimental aggregate was always kept at atmospheric pressure (Leffelaar 1986), this was also done in the simulation.

Computer program

Numerical calculations were done by a program written in Continuous System Modeling Program III (CSMP III) language (IBM 1975) and executed on a VAX machine. The program was developed and written with two targets in mind (apart from simulating the processes of respiration and denitrification in the unsaturated soil aggregate): (1) to facilitate the communication of the model and the very large program to others; (2) to minimize programming errors. Therefore, the calculation sequence has been summarized in terms of calls to (FORTRAN) subroutines in the main (CSMP) program. The main program contains three major sections: (1) a parameter section, summarizing all biological, soil physical, chemical, and runtime control parameters; (2) an initial section, mainly to calculate the amounts of the state variables at time zero, and to convert a number of parameters to SI units and to 20°C; all actual input parameters for the dynamic section are printed for control purposes; (3) a dynamic section, starting with the state variables in terms of amounts contained in integrals. The latter is followed by subsections to calculate: (a) derived quantities from the state variables (material balances, concentrations, gradients, conductivities, diffusion coefficients, and reduction factors due to tortuosity); (b) production terms; (c) gross rates of change of each integral value; and (d) net rates of change for each integral value. A last subsection contains the routines for printing results. The types of subroutines that are called from the dynamic section can be classified similarly to the subsections distinguished there. In addition, however, subroutines that contain only the control structures to choose the correct calculation subroutines, i.e., on the basis of the actual environmental conditions, are distinguished. Thus, the extensively structured program enables one to get a quick overview of the calculations, whereas details may be studied in the separate subroutines. Care has been taken to maintain the recognizability of the rate equations in the subroutines. The program contains 120 subroutines and 110 pages of code. Process descriptions of respiration and denitrification, gas transport, water transport, and solute transport take about 20, 55, 20, and 5% of the program code, respectively. The simulations reported in this work took about 100 and 300 min of CPU time on a VAX-8700 and VAX-785 machine, respectively, for a 45-h real-time simulation. Few comments have been given in the program code, except for the subroutines that contain the control structures. Instead, units and abbreviations of all variables and short subroutine descriptions have been given in a separate listing (45 pages). A system to abbreviate variables was designed and applied to improve the recognizability of the variables and the readability of the program.

All results presented were obtained by the variable time-step-integration method of Runge-Kutta Simpson, which is especially provided for continuous processes. During a simulation, however, discontinuities in total gas pressure may occur when a layer has become gas-continuous. At such events and when the preceding integration is successfully completed, as indicated by the CSMP integration status variable, the pressure adjustment algorithm is executed, and the values of the state variables in the integrals are adjusted. Just before and after the adjustment procedure, the values of the gas pressures and concentrations in the aggregate layers and in the chamber that contained the aggregate, are printed in a separate file for control purposes. Material balances of water, nitrogen, and carbon were computed during the simulation runs and were found to be correct. To prevent adverse numerical effects of the occurrence in the simulations of slightly negative amounts or concentrations of substances that were consumed, small (<0.5% with respect to the maximum of the variable) threshold values were introduced. Below these threshold values, the appropriate consumption rates were set to zero. The program gives results in terms of rates of respiration and denitrification; fluxes of gases, water, and substrates; concentrations of biomass (with respect to dry soil mass), water (with respect to volume of soil), and substrates (with respect to volume of water); and concentrations and pressures of gases in the aggregate layers and in the chamber that contains the aggregate.

Model parameters

The procedure followed to come to a judgment about the simulation model was similar to the one proposed by Leffelaar and Wessel (1988): data not measured during the present study we gathered from different authors, and we then investigated whether it was possible to simulate the overall picture of the experiment by modifying some of the gathered data within reasonable limits.

Pertinent data of aggregate

The initial volume of the chamber that contained the aggregate for the reported experiment was 530 cm^3.

Aggregate dimensions were those of the experimental system: height and diameter 2.59 and 9.8 cm, respectively (Leffelaar 1986). Fourteen concentric layers were distinguished to characterize the space coordinate of the model aggregate: five layers of 0.2 cm, two of 0.3 cm, two of 0.4 cm, and five of 0.5 cm. The choice of both number and grouping of layers was based on a compromise between the need to simulate the expected large gas concentration gradients in the wet outer soil layers with reasonable accuracy and to optimize the time step used for the Runge-Kutta Simpson integration method both with respect to maintaining numerical stability and to minimizing roundoff errors in this single-precision integration algorithm. Soil porosity, 0.478 cm^3 cm^{-3}, was calculated from the volume and amount of soil, using a particle density of 2.65 g cm^{-3}. Gas pressures in the soil layers and in the chamber that contained the aggregate were initiated according to the gas composition used to flush the respirometer system (Leffelaar 1986): 19.525 kPa and 81.8 kPa for oxygen and neon, respectively. The amount of solution added to the aggregate at the start of the simulation was 43.2 cm^3; it contained 3.0 g/L of glucose and 8.44 g/L of potassium nitrate, so that the amounts of C and N applied were similar to those in the experiment.

Microbiological characteristics

Microbiological parameters for bacteria that can grow with oxygen as electron acceptor under aerobic conditions or with nitrate, nitrite, and nitrous oxide as electron acceptor under anoxic conditions (subsequently called *denitrifiers*) were discussed by Leffelaar and Wessel (1988) with respect to anoxic conditions. The data reported in their Table 2 (column 5) with respect to biomass concentration ([B]), maximum relative growth rates (μ), half-saturation values (K), maximum growth yields (Y), and maintenance coefficients (m) on different electron acceptors were used as a starting point in the present study; these data are not repeated here. The data could not be used directly because, unfortunately, Leffelaar and Wessel (1988) used loam soil from Herveld, whereas Leffelaar (1986) used sandy loam soil from Lelystad. After some preliminary simulation runs, it appeared that reasonable results were obtained with respect to the experimental data (Leffelaar 1986), when [B] was set at 10^{-5} kg C per kg of dry soil (0.1), the initial mass fraction of denitrifiers with respect to total biomass (F_{den}) was set at 0.8 (40), and the maximum growth yield, Y, on nitrate and nitrite was set at 0.025 (0.25) and 0.214 (4), respectively, where bracketed numbers indicate the factors with which the data of Leffelaar and Wessel (1988) were multiplied to arrive at the present data. Other previously reported microbiological parameters remained unchanged.

Maximum relative growth rates with oxygen as electron acceptor are needed for both the bacteria that can grow only with oxygen as electron acceptor (subsequently called *strict aerobes*) and the denitrifiers. As a first estimate for both groups of bacteria, this value was taken equal to the sum of the maximum relative growth rates on the nitrogenous electron acceptors, i.e., 0.75 10^{-5} s^{-1}.

A half-saturation value (K) for oxygen respiration in water-saturated soil crumbs was reported by Greenwood (1961): 10^{-3} mol O_2 m^{-3} H_2O. This value was used for the aerobic respiration of the strict aerobes. The half-saturation values on glucose for strict aerobes and denitrifiers under aerobic conditions were taken similar to the value for the denitrifiers under anaerobic conditions: 0.0174 kg C m^{-3} H_2O (Shah and Coulman 1978).

Maximum growth yields, Y, and maintenance coefficients, m, on glucose as carbon source and oxygen as electron acceptor are needed in the model. Van Verseveld et al. (1977) and Meijer et al. (1977) reported values for *Paracoccus denitrificans* grown in continuous culture under, respectively, anaerobic and aerobic conditions on gluconate ($C_6H_{12}O_7$) as carbon source and nitrate or oxygen as electron acceptor. Y_c and

m_c values in both studies were very similar. Therefore, the values for glucose under aerobic conditions were taken identical to those under anaerobic conditions: 0.503 kg B kg^{-1} C and 0.212 10^{-5} kg C kg^{-1} B s^{-1}. The values used for Y_{O2} and m_{O2} were 0.65 kg B kg^{-1} O_2 and 0.382 10^{-5} kg O_2 kg^{-1} B s^{-1}, respectively. These values were obtained by converting the values reported by Meijer et al. (1977), using the elementary composition of *Paracoccus denitrificans* as explained previously (Leffelaar and Wessel 1988). After the preliminary simulation runs a value of 0.16 kg B per kg O_2 was adopted for Y_{O2}: this is the value of Meijer et al. (1977) multiplied with the ratio (0.25) of the sum of the maximum growth yields on nitrogenous compounds as used in the present study to the sum of the literature compilation by Leffelaar and Wessel (1988, their Table 2, fourth column).

The mineralization parameters, F_c and F_n, were taken 0.6 under aerobic conditions.

The oxygen pressures that delimit the transition zone where denitrifiers may utilize both oxygen and nitrogenous compounds as electron acceptor were 101 ($[O_2]_l$) and 1013 ($[O_2]_h$) Pa, respectively (Leffelaar 1987).

Hydraulic characteristics

Initial water distribution was given by the water content measurement at the start of the experiment reported previously (Leffelaar 1986); it is reproduced here in Fig. 4 in the section about results and discussion. The main water retention curves and the hydraulic conductivity curves for the sandy loam soil from Lelystad are depicted in Fig. 3. The data points for the main water-retention curves were obtained for uniformly packed soil samples contained in Perspex rings (diameter and height 2.7 and 1 cm, respectively) of which the bottom was closed by gauze. The soil used was pulverized to pass a 0.5-mm sieve, similar to the soil used to prepare the experimental aggregate (Leffelaar 1986). Soil pressure heads for the desorption curve were applied using a Blokzijl sand box (0, 10, 31.5, and 100 cm), a kaolin box (270, 520, and 1000 cm), and a pressure membrane apparatus (16 000 cm) according to procedures described by Stakman (1974). Soil water pressure heads for the main sorption curves were started at a pressure head of 520 cm using initially air-dry soil. Treatments were quintupled. The dashed water retention curves in Fig. 3 were

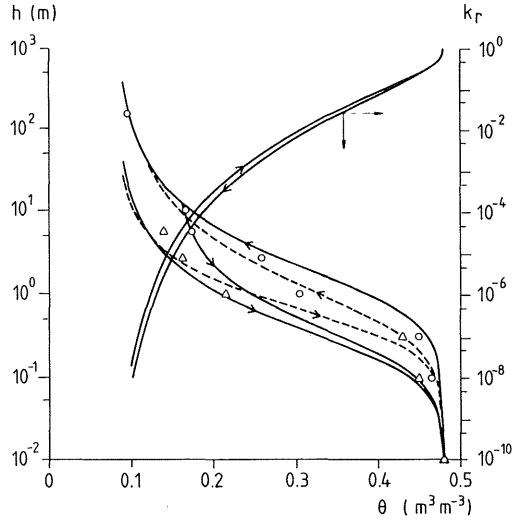

FIG. 3. Experimental (○: desorption; △: sorption), curve-fitted (-----, van Genuchten 1978), and hand-drawn envelope (——) soil water retention curve that produced the best agreement between measured and simulated water contents, and primary wetting scanning curve used for initiation of model; calculated (— —, van Genuchten 1978) relative hydraulic conductivity curves based on hand-drawn water retention curves, for Lelystad sandy loam.

obtained by the optimization procedures by van Genuchten (1978); the continuous hand-drawn envelope curves produced the best agreement between measured and simulated water contents, however. Therefore, these were used to produce the data presented below. Assuming that the aggregate followed the main drying curve before the solution was added, initiation of pressure head in each compartment was carried out according to the primary wetting scanning curve that is also shown in Fig. 3. To calculate the scanning curves, a hyperbolic type of equation, $y = a/(|\theta - \theta_T| + a)$, was used (Dane and Wierenga 1975): when the difference between the water content where a reversal from, for example, drying to wetting occurs (θ_T) and the actual water content (θ) equals a, the scanning curve is halfway between the main water retention curves. The pressure head at the actual water content is then given by the sum of the pressure head at the main drying curve times y, and the main wetting curve times $(1 - y)$. Parameter a in the hyperbola was taken 0.01 m^3 m^{-3} (Dane and Wierenga 1975).

The hydraulic conductivity-water content curves in Fig. 3 were calculated from the enve-

lope water retention curves by procedures outlined by van Genuchten (1978): these calculations gave the relative hydraulic conductivity curves, however, and a matching point was needed, e.g., the saturated hydraulic conductivity. Saturated hydraulic conductivity was obtained using similarly prepared soil samples as used for the water retention curves in small Perspex cylinders (diameter and height 1.6 and 10 cm, respectively), following the constant-head method described by Kessler and Oosterbaan (1974). The value obtained, 5 10^{-7} m s^{-1}, was determined in quadruplicate. The preliminary simulation runs showed that the rate of water redistribution hardly affected the course of other processes, because gas continuity between the aggregate and the surroundings did not occur at the final water distribution. Therefore, solely to reduce computer time, the saturated hydraulic conductivity was taken 5 times smaller.

Transport characteristics in the water phase

Diffusion coefficients for nitrate and glucose at 25°C were 19 10^{-10}, and 6.7 10^{-10} m^2 s^{-1}, respectively (Harremoës 1978). (Correction of data to 20°C would not exceed 3%, and was neglected.) The value for nitrite was not reported; it was taken equal to the one for nitrate.

Diffusion coefficients at about 20°C for oxygen, carbon dioxide, and molecular nitrogen in water were 20 10^{-10}, 16.5 10^{-10}, and 22 10^{-10} m^2 s^{-1}, respectively (Harremoës 1978). The values for nitrous oxide and neon were not reported; they were taken equal to those of carbon dioxide and molecular nitrogen because of their respective similarities in molecular weights. From the preliminary simulation runs it appeared that hardly any gaseous exchange between the interior of the aggregate and the surroundings occurred when these literature data were used. The experimental findings (Leffelaar 1986), however, showed that exchange of gases between the aggregate and the surroundings was much more pronounced. Therefore, assuming that gaseous transports through the water phase of soil were well described, it seems probable that in the experimental aggregate these transports were enhanced, e.g., through small cracks in the outer part of the aggregate. In an attempt to take account of this enhancement in gaseous exchange, the diffusion coefficients of gases in water were set 10 times higher compared with the literature values for pure water. Gas solubility coefficients at 20°C and 1 atm for oxygen, carbon dioxide, nitrous oxide, molecular nitrogen, and neon were reported by Wilhelm et al. (1977): 0.033, 0.937, 0.679, 0.017, and 0.011 m^3 gas m^{-3} water, respectively. The relationship between the tortuosity factor for diffusion of solutes and gases in the water phase and soil water content were taken from a literature compilation by Leistra (1978): values for λ_w were 0.03, 0.1, 0.2, 0.34, and 0.5 for θ values of 0.1, 0.2, 0.3, 0.4, and 0.5 m^3 m^{-3}, respectively. The value for the dispersion length (L_d) for this fine-packed soil was suggested by Prof. G. H. Bolt (personal communication): 0.001 m.

Transport characteristics in the gas phase

Parameters and equations needed to calculate binary diffusion coefficients were reported previously (Leffelaar 1987). The resulting values for D_{iNe} at 20°C and atmospheric pressure were: 0.32 10^{-4}, 0.24 10^{-4}, 0.24 10^{-4}, 0.31 10^{-4}, and 0.49 10^{-4} m^2 s^{-1} when i stands for oxygen, carbon dioxide, nitrous oxide, molecular nitrogen, and neon, respectively. As a first approximation, the tortuosity factor for diffusion of gases in the gas phase, λ_g, was represented by the same relationship as the one used for solutes in the water phase: for the gases it was related to the gas-filled porosity, however. The value for the gas-filled porosity where soil was considered gas-continuous, ε_g^{crit}, was taken 0.063 m^3 m^{-3}. This value was simply just sufficient to prevent gas continuity throughout the aggregate. The preliminary simulations showed that when ε_g^{crit} was taken slightly smaller, gas continuity occurred, anaerobiosis quickly disappeared, and denitrification ceased: such results were contradictory to the experimental findings (Leffelaar 1986), and it was thus concluded that no gas continuity had occurred in the experiment. The value of about 6% for the critical gas-filled porosity was near to experimental values found by Le Van Phuc and Morel-Seytoux (1972) and Corey (1957).

RESULTS AND DISCUSSION

A representative experimental data set on the distribution of water, gases, and nitrogen species was discussed by Leffelaar (1986). Present simulation results are compared with that particular data set in Figs. 4 through 7. The experimental results from Leffelaar (1986) are represented by

the smooth curves as previously drawn through the data points. Actual data points have been omitted here to improve readability of the figures; for an assessment of the quality of experimental curves and data points, reference is made to the original paper.

Figure 4 shows the volumetric water distribution at the start of the simulation and at the end, after 45 h: simulated redistribution was essentially completed after 12 h. Simulated curves are not smooth, because plotted water contents were obtained by weighing and summing the water contents of the concentric layers that coincided with a measuring location: thus plotted data refer to the rectangular geometry of the water measurements obtained by gamma radiation (de Swart and Groenevelt 1971). The major portions of the simulated and experimental curves match very well. The simulated curve at 45 h was fully determined by the initial water-distribution and the water-retention curves shown in Fig. 3. At the outside of the aggregate, however, the simulated water content is about 1 to 3% lower than the experimental value, and consequently the air-filled porosity at the outside was that much higher. The critical air-filled porosity in the simulation was so chosen that no gas continuity would occur after redistribution of water, in accordance with the experimental findings. When the critical air-filled porosity

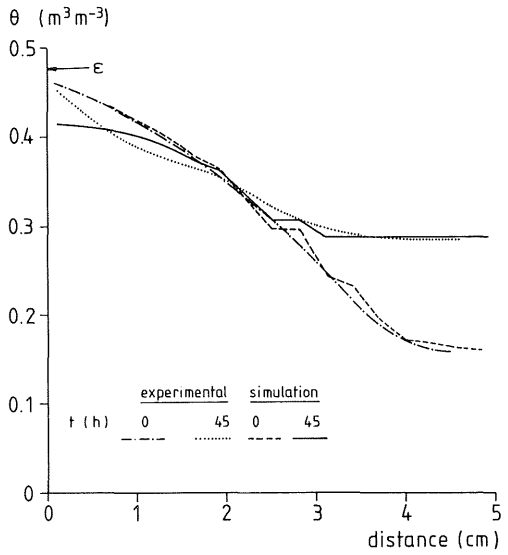

FIG. 4. Simulated and experimental volumetric water distribution in soil aggregate (center at distance 4.9 cm) at time zero and after 45 h.

was taken slightly lower, however, the aggregate became gas-continuous, anaerobiosis disappeared quickly, and denitrification ceased. It thus appears that air-filled porosity is a determining factor in the regulation of oxygen status of soil and with this in the regulation of denitrification.

Figure 5 shows oxygen pressures (left y axis) in the aggregate center and the periphery to equal about zero after 14 h. The oxygen pressure curves show satisfactory similarity to the experimental findings. (The experimental results of peripheral (dotted line) and central (short-dash line) electrodes coincided up to about 10 h; after about 14 h the experimental results of the central electrode coincided with the simulated results.) The simulated results show an interesting feature of the model: when the layer where the peripheral oxygen electrode is located becomes gas-continuous, a pressure jump occurs. This feature has a number of aspects. First, the oxygen pressure in the layer that has become gas-continuous was ahout 4 kPa lower than in the adjacent series of gas-continuous layers before the pressure jump occurred; hardly any gradient in oxygen pressure occurred in the adjacent series of layers. Thus, gaseous transport through the water phase was very limited. Second, this jump or a more gradual change in oxygen pressure was not found in the experimental results. Therefore, it is very probable that gas-continuity has been present in the layers where the oxygen electrodes were located in the experiment, resulting in similar electrode readings. Third, such pressure jumps focus attention on the practical problem of measuring oxygen pressure by polarographic Clark-type oxygen electrodes (Leffelaar 1986). The calculated absolute pressure in the layer that has become gas-continuous was 86.9 and 103.9 kPa before and after the jump, respectively. Because changes in absolute pressure cause proportional changes in oxygen pressure, Clark-type oxygen electrode measurements will be directly affected (Fatt 1976). The simulated results were obtained using diffusion values for gases in water that were 10 times higher than those reported in the literature, to take account of possible enhancement of gaseous exchange between the aggregate and the surroundings, as explained in the section about model parameters. When the literature values were used, however, the results of the oxygen electrodes were hardly affected after the

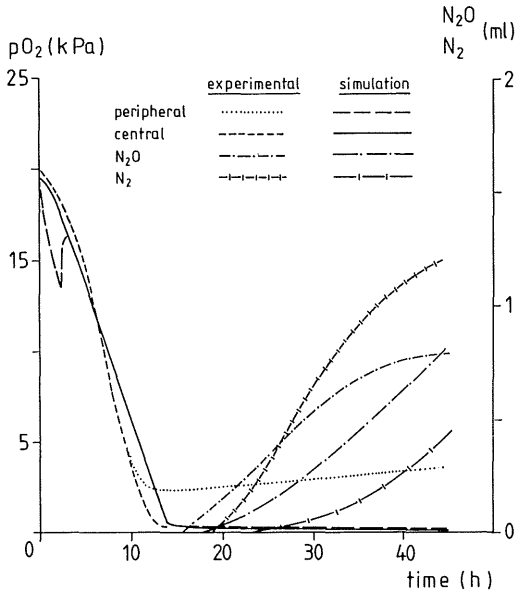

FIG. 5. Simulated and experimental oxygen pressure (left y axis) in center and 4 cm from center (peripheral) of soil aggregate and volumes of nitrous oxide and molecular nitrogen in chamber that contains the aggregate (right y axis) as a function of time.

pressure jump; before that moment, oxygen pressure at the location of the peripheral electrode had decreased to 11.5 kPa instead of 13.4 kPa (Fig. 5). This result would mean that the time course of the oxygen pressure is mainly determined by the actual soil respiration rate and the amount of oxygen present at time zero, and to a lesser extent by gaseous transport through the water phase.

Figure 6 shows that the oxygen outside the aggregate decreased much slower than in the experiment. Oxygen decrease will be determined by the respiration rate and the volume of the aerobic outer shell of the aggregate, Fig. 1b. Introducing higher aerobic respiration rates in an attempt to better match the experimental decrease of oxygen in the soil container, however, caused a proportionally faster decrease of the oxygen pressures at the locations of the electrodes. Thus, the enhancement in gaseous exchange between the aggregate and the surroundings was stronger than represented by the 10 times higher diffusion coefficients in the water phase, and a greater part of the soil volume did participate in oxygen respiration in the experiment. The ratio of oxygen flux density at 21 h in the experiment (2.7 L O_2 m^{-2} d^{-1}, Leffelaar (1986) to that of the simulation (0.61 L O_2 m^{-2} d^{-1}) would suggest that the order of magnitude of the aerobic shell in the experiment was about four times larger compared with the simulation. Because oxygen penetration in the simulation equaled about 0.2 cm, this would mean that in the experiment oxygen penetrated into the aggregate to a depth of about 0.8 cm. This is very near to the peripheral electrode, which in fact stabilized at about 2 kPa in the experiment, Fig. 5.

Figure 6 also shows the development of carbon dioxide. It is seen that the simulated curve lags behind compared with the experimental one, as in the case of the oxygen curve. This will be caused in part by the low carbon dioxide transport rate and in part by a similar reasoning as in the case of oxygen: due to low gas-transport rates, the aerobic soil volume participating in aerobic respiration will be smaller, and thus carbon dioxide production under aerobic conditions will be lower, and a smaller amount of this gas is transported into the soil container. Though the simulated curve lags behind compared with the experimental one, it is near complementary to the simulated oxygen curve, resulting in a respiration quotient of about 1. In fact, the respiration quotient behaved as a

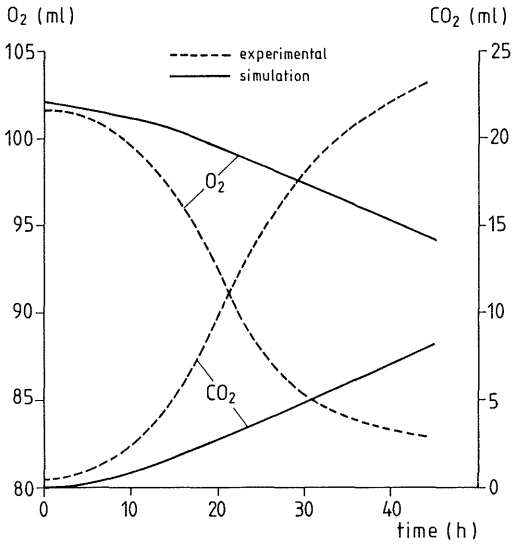

FIG. 6. Simulated and experimental volumes of oxygen (left y axis) and carbon dioxide (right y axis) in chamber that contains the aggregate as a function of time.

damped oscillation (0.4 (1 h) → 1.27 (8 h) → 1.44 (12 h) → 0.97 (23 h) → 1.0 (28 h)) and stabilized after 28 h. A respiration quotient of 1 was also found in the experiment (Leffelaar 1986). One would expect higher final values, however, because the whole of the aggregate was producing carbon dioxide, and only the outer shell consumed oxygen. When the literature values of the gas diffusion coefficients were used, the sequence of respiration quotients was (0.4 (1 h) → 0.6 (3 h) → 0.9 (11 h) → 1.66 (16 h) → 2.44 (45 h)), and no stabilization occurred. These simulated findings demonstrate a strong influence of transport processes on the respiration quotient of soil. Furthermore, the conclusion that the respiration quotient is not a sensitive measure to decide whether a soil is partially anaerobic, as suggested earlier on the basis of experimental results (Leffelaar 1986), is supported by these theoretical findings. The discrepancy between a respiration quotient of about 1 and the knowledge that soil is partially anaerobic was previously ascribed to the higher solubility of CO_2 in water compared with O_2, with the expectation that CO_2 would be released slower from the soil than O_2. As a consequence, the respiration quotient would be underestimated as long as no steady rates of exchange of CO_2 and O_2 were established (Leffelaar 1986). The above reasoning was not confirmed by theory: a simulation where the solubility of carbon dioxide in water was set 10 times smaller than the literature value revealed that the respiration quotient was about halved before steady rates of exchange of CO_2 and O_2 were established. After 28 h it stabilized at about 1 again.

Production of nitrous oxide and molecular nitrogen is shown in Fig. 5. The simulated curves lag behind compared with the experimental curves for reasons similar to those previously discussed for oxygen and carbon dioxide. The flux densities of nitrous oxide and molecular nitrogen at 40 h, however, equaled 1.4 and 1.1 kg N ha^{-1} d^{-1}, which was rather similar to the experimental values: 1.3 and 1.9 kg N ha^{-1} d^{-1}, respectively. The curves of the development of nitrous oxide and molecular nitrogen did not decrease as suggested by the experimental curves. On second thought, this suggestion might be misleading, for much nitrite, and some nitrate, was still found inside the experimental aggregate, and denitrification probably continued (Leffelaar 1986). The linear increase of nitrous oxide and the curvilinear increase of molecular nitrogen with time in the simulation can be explained by the fact that the pressure of nitrous oxide hardly changed inside the aggregate after 30 h, while that of molecular nitrogen increased by about 0.3 to 0.4 kPa per hour: thus the driving force for diffusive transport for N_2O remained similar, while that of N_2 increased.

Figure 7 depicts the simulated and measured distributions of nitrate and nitrite in the soil aggregate after 45 h. The calculated nitrate distribution deviates strongly from the measured distribution: simulated concentrations decrease from outside to the center of the aggregate, whereas experimental concentrations increase. Note, however, that the model results are consistent with the assumption that reduction of nitrate due to denitrification will be less in regions where oxygen is present, i.e., the outer shell of the aggregate. In this respect the experimental results were rather unexpected: nitrate was depleted in a region where oxygen could probably penetrate (see above discussion with respect to oxygen in Fig. 6). It might be that the upper limit of oxygen pressure below which both denitrification and oxygen consumption may take place was actually higher in the experiment,

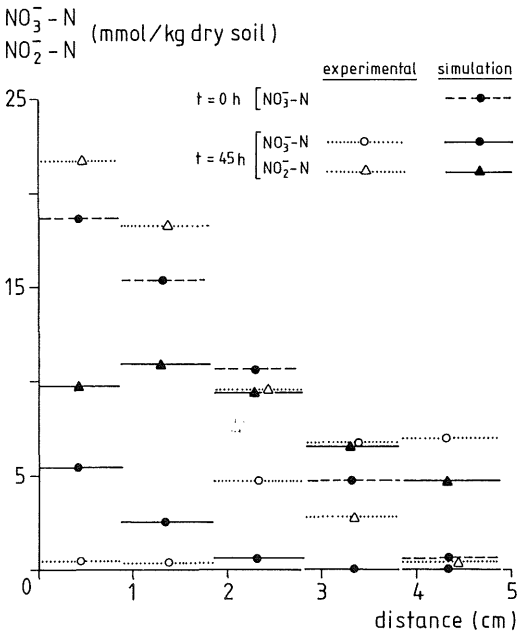

FIG. 7. Simulated and experimental distributions of nitrate and nitrite in soil aggregate (center at distance of 4.9 cm) at time zero and after 45 h.

causing more nitrate to be denitrified in the outer shell. The picture of the calculated nitrite concentrations resembled the measured data better. The influence of water redistribution on the simulated nitrite concentration is demonstrated in the center of the aggregate, where nitrite-N is much higher than the initial nitrate-N concentration. Thus either nitrate was leached into the center and subsequently denitrified to nitrite, or nitrite formed in adjacent soil layers was transported to the center.

CONCLUSIONS

We concluded from the above discussion that the simulation model presented gives a satisfactory description of the soil biological system studied: part of the experimental results could be described quantitatively, e.g., water distribution and the time course of the oxygen pressure at the experimental positions of the electrodes, whereas other data that deviated from the experimental data, e.g., consumption rate of oxygen and production rates of carbon dioxide, nitrous oxide, and molecular nitrogen, could be understood by studying the dynamic behavior of the model.

The model gives rise to the following conclusions about a number of physical soil properties that are usually not measured or considered in soil physics literature with respect to biological processes in soil:

1. The critcal gas-filled porosity below which gaseous transport takes place through the water phase is a determining factor in gaseous exchange in soil.

2. Soil water hysteresis is important in causing a nonhomogeneous soil water distribution at a homogeneous pressure head distribution, implying that a small amount of added water is sufficient to decrease the gas-filled porosity to values smaller than the critical gas-filled porosity.

3. The rate at which water redistributes hardly affects the course of the biological processes if the final water distribution does not allow for gas-continuity between aggregate and surroundings.

4. The rate of water distribution is very important, however, if gas-continuity does occur during the redistribution process. Then, this rate determines the time period in which anaerobiosis and possibly denitrification can occur.

5. Soil respiration may cause differences in soil atmospheric pressure on the order of magnitude of ±10% in the enclosed gas-continuous part of the soil, which may affect soil hydraulic characteristics (Chahal 1966).

6. The exchange of gases between aggregate and surroundings is seriously underestimated when it is fully ascribed to diffusion through the water phase of gas-discontinuous soil layers: the model suggests that enhancement of gas exchange occurs, perhaps through small cracks in the outer part of the aggregate.

7. Total gas pressure jumps, as simulated by the model, will affect the measurement of oxygen pressure by polarographic oxygen electrodes, though it remains to be investigated whether such pressure jumps will actually occur in field soil.

This study showed that the parameterization of the model formed the major problem that needs attention first. Therefore, a more extensive exploration of both the experimental respirometer system (Leffelaar 1986) and the theoretical simulation model is intended for the near future: the model will be used first to plan experiments with respect to the respirometer system, second to help interpret the data so obtained, and third to investigate the relative importance of a number of parameters in a sensitivity analysis.

Finally, we concluded that only the interaction between experiment and theory will ultimately lead to a full understanding of the complex soil biological system described.

ACKNOWLEDGMENTS

I wish to thank Ir. J. H. G. Verhagen and Dr. J. Goudriaan for their indispensable help in developing the equations to maintain equal total gas pressures in adjacent gas-continuous soil layers. Mr. A. J. Koster and Mr. G. Klein of the computer center of the university were kind to provide the necessary memory space and CPU time to execute the program on the VAX. I also thank Mr. E. Korzilius for determining the hydraulic characteristics of the Lelystad soil and for developing the preliminary version of the soil water submodel. Mr. C. Rijpma skillfully prepared the figures. Prof. G. H. Bolt, Prof. C. T. de Wit, and Ir. J. H. G. Verhagen reviewed the manuscript.

LIST OF SYMBOLS

Symbol	Meaning	Unit
a	half transition constant in hysteresis hyperbola: when $\lvert \theta - \theta_T \rvert = a$, half the transition to the main drying or wetting curve is completed	$m^3\ m^{-3}$
$A(l)$	interfacial total soil area between adjacent layers; index refers to interface with previous layer	m^2
$Am(g, l)$	amount of gas g in layer l	mol
$A_p(l)$	amount of gas transferred to adjust the pressure in layer l to that of adjacent layers; index refers to interface with previous layer	mol
B	amount of bacterial carbon. Refers either to strict aerobes or denitrifiers	kg C
$[B]$	concentration of bacterial carbon. Refers either to strict aerobes or denitrifiers	kg C kg^{-1} dry soil
c_i	concentration of substance i. When $i = g$, it refers to gas, and units are either mol m^{-3} of gas phase or mol m^{-3} H_2O; when $i = s$, it refers to solute, and unit is kg m^{-3} H_2O	amount m^{-3}
$c, c(l)$	total molar gas concentration in general, $c = \sum_g c_g$, and with respect to layer l, respectively	mol m^{-3}
$c(g, l)$, $c'(g, l)$	molar concentration of gas g in layer l; second concentration is defined by Eq. (7) and it is included in first concentration, Eq. (10)	mol m^{-3}
C_i	concentration of substance i with respect to volume of soil. When $i = g$, it refers to gas, and amount is mol; when $i = s$, it refers to solute, and amount is kg; when $i = w$, it refers to water, and amount is m^3 H_2O. Symbol is used only in the equation of continuity, Eq. (1)	amount m^{-3} of soil
D_0	diffusion coefficient of solute or gas in free liquid water	$m^2\ s^{-1}$
D_{ij}	binary diffusion coefficient of gas pair $i - j$ in free air	$m^2\ s^{-1}$
F_c, F_n	mass fraction of carbon and nitrogen that mineralizes from the dead biomass	–
F_{den}	initial mass fraction of denitrifiers with respect to total bacterial biomass	–
h	pressure head of soil water. h is a function of volumetric water content	m
h	subscript referring to high critical level	
J_i	flux of substance i. When $i = g$, it refers to gas, and amount is mol; when $i = s$, it refers to solute, and amount is kg; when $i = w$, it refers to water, and amount is m^3 H_2O	amount m^{-2} s^{-1}
$J(g, l)$	molar flux of gas g into layer l	mol m^{-2} s^{-1}
$J_p, J_p(l)$	pressure adjustment flux in general and for the gas flux into layer l, respectively; index l refers to interface with previous layer	mol m^{-2} s^{-1}
$J_w(l)$	flux of water into layer l	$m^3\ m^{-2}\ s^{-1}$
k	hydraulic conductivity. k is a function of volumetric water content	m s^{-1}
K	half-saturation value with respect to carbon or electron acceptor	kg m^{-3} H_2O
$K(g)$	gas solubility coefficient in liquid water at 20°C and 1 atm	m^3 gas m^{-3} H_2O
l	subscript referring to low critical level or bracketed index to indicate layer number	
L_d	dispersion length parameter	m
m, m_c	maintenance coefficients with respect to carbon or electron acceptor and for carbon specifically, respectively	kg kg^{-1} B s^{-1}
p	pressure	Pa

P_i	net production term of substance i. When $i = g$, it refers to gas, and amount is mol; when $i = s$, it refers to solute, and amount is kg. For a gas in layer l: $P_g = S(g, l)/V(l)$	amount m^{-3} s^{-1}
R	gas constant	Pa m^3 mol^{-1} K^{-1}
$S(g, l)$	gas production term of gas g in layer l	mol s^{-1}
t	time	s
T	absolute temperature	K
$V(l)$	volume of a soil layer, i.e., sum of volumes of gas, water, and solids	m^3
$V(g, l)$	gas volume occupied by gas g in layer l with reference to both gas and water phases. $V(g, l)$ is defined by Eq. (8)	m^3
x	space coordinate	m
y	weight factor: outcome of hyperbolic equation that forces a scanning curve toward one of the main water retention curves ($0 \leq y \leq 1$)	–
Y, Y_c	maximum growth yield on carbon or electron acceptor and on carbon specifically, respectively, when no substrate would be used for maintenance	kg B kg^{-1}
Δ	finite difference of concerning symbol	
ε, ε_g, $\varepsilon_g(l)$	total soil porosity and actual volumetric gas content in general and in layer l, respectively: $\varepsilon_g = \varepsilon - \theta$	m^3 m^{-3}
ε_g^{crit}	critical gas content where gas phase in layers is just discontinuous	m^3 m^{-3}
θ, $\theta(l)$, θ_T	volumetric water content in general, in layer l and at a transition point on wetting or drying curve where scanning drying or scanning wetting curve starts, respectively	m^3 m^{-3}
λ_i	tortuosity factor. When $i = w$, tortuosity in water phase; when $i = g$, tortuosity in gas phase. λ_w and λ_g are functions of θ or ε_g, respectively	–
μ	maximum relative growth rate on oxygen with glucose C as carbon source	s^{-1}
$\sum$	summation operator	
$\lvert\ \rvert$	bars around a variable means absolute value	
$^-$	superscript; linearly interpolated spatial average of concerning symbol with respect to the layer in brackets and the previous one	

REFERENCES

Bolt, G. H. 1979. Movement of solutes in soil: Principles of adsorption/exchange chromatography. *In* Soil chemistry B. Physico-chemical models. G. H. Bolt (ed.). Developments in Soil Science, 5B. Elsevier, Amsterdam, pp. 285–348.

Chahal, R. S. 1966. Effect of entrapped air and pressure on matric suction. Soil Sci. 102:131–134.

Corey, A. T. 1957. Measurement of water and air permeability in unsaturated soil. Soil Sci. Soc. Am. Proc. 21:7–10.

Currie, J. A. 1961. Gaseous diffusion in the aeration of aggregated soils. Soil Sci. 92:40–45.

Dane, J. H., and P. J. Wierenga. 1975. Effect of hysteresis on the prediction of infiltration, redistribution and drainage of water in a layered soil. J. Hydrol. 25:229–242.

Delwiche, C. C. 1981. The nitrogen cycle and nitrous oxide. *In* Denitrification, nitrification, and atmospheric nitrous oxide. C. C. Delwiche (ed.). Wiley, New York, pp. 1–15.

Fatt, I. 1976. Polarographic oxygen sensors. CRC Press, Cleveland, Ohio, p. 278.

Frissel, M. J., and P. Reiniger. 1974. Simulation of accumulation and leaching in soils. Simulation Monographs, PUDOC, Wageningen, The Netherlands, p. 116.

Genuchten, M. Th., van. 1980. A closed-form equation for predicting the hydraulic conductivity of unsaturated soils. Soil Sci. Soc. Am. J. 44:892–898.

Genuchten, R., van. 1978. Calculating the unsaturated hydraulic conductivity with a new, closed-form analytical model. Research Report 78-WR-08, Water Resources Program, Dept. of Civil Engineering, Princeton Univ., Princeton, N.J.

Goudriaan, J. 1973. Dispersion in simulation models of population growth and salt movement in the soil. Neth. J. Agric. Sci. 21:269–281.

Greenwood, D. J. 1961. The effect of oxygen concentration on the decomposition of organic materials in soil. Plant Soil 14:360–376.

Harremoës, P. 1978. Biofilm kinetics. *In* Water pollution microbiology, vol. 2. R. Mitchell (ed.). Wiley, New York, pp. 71–109.

Hopmans, J. W., and J. H. Dane. 1986. Combined effect of hysteresis and temperature on soil-water movement. J. Hydrol. 83:161–171.

IBM Corp. 1975. Continuous system modeling program III (CSMP III). Program reference manual. SH 19-7001-3. Data Processing Division, 1133 Westchester Ave., White Plains, N.Y.

IMSL. 1982. International mathematical and statistical libraries, Inc. Reference manual, edition 9. Customer relations, 6th floor, NBC Building, 7500 Bellaire Blvd., Houston, Tex.

Ingraham, J. L. 1981. Microbiology and genetics of denitrifiers. *In* Denitrification, nitrification, and atmospheric nitrous oxide. C. C. Delwiche (ed.). Wiley, New York, pp. 45–65.

Kessler, J., and R. J. Oosterbaan. 1974. Determining hydraulic conductivity of soils. *In* Drainage principles and applications: 3. Surveys and investigations. ILRI, Wageningen, The Netherlands, pp. 253–296.

Kool, J. B., and J. C. Parker. 1987. Development and evaluation of closed-form expressions for hysteretic soil hydraulic properties. Water Resour. Res. 23:105–114.

Koorevaar, P., G. Menelik, and C. Dirksen. 1983. Elements of soil physics. Developments in Soil Science, 13. Elsevier, Amsterdam, p. 228.

Leffelaar, P. A. 1979. Simulation of partial anaerobiosis in a model soil in respect to denitrification. Soil Sci. 128:110–120.

Leffelaar, P. A. 1986. Dynamics of partial anaerobiosis, denitrification, and water in a soil aggregate: Experimental. Soil Sci. 142:352–366.

Leffelaar, P. A. 1987. Dynamic simulation of multinary diffusion problems related to soil. Soil Sci. 143:79–91.

Leffelaar, P. A., and W. Wessel. 1988. Dentrification in a homogeneous, closed system: Experiment and simulation. Soil Sci. 146: 335–349.

Leistra, M. 1972. Diffusion and adsorption of the nematicide 1,3-dichloropropene in soil. PUDOC, Wageningen, The Netherlands, p. 105.

Leistra, M. 1978. Computed redistribution of pesticides in the root zone of an arable crop. Plant Soil 49:569–580.

Leistra, M. 1980. Transport in solution. *In* Interactions between herbicides and the soil. R. J. Hance (ed.). Academic Press, London, pp. 31–58.

Leistra, M., R. H. Bromilow, and J. J. T. I. Boesten. 1980. Measured and simulated behavior of oxamyl in fallow soils. Pestic. Sci. 11:379–388.

Le Van Phuc, and H. J. Morel-Seytoux. 1972. Effect of soil air movement and compressibility on infiltration rates. Soil Sci. Soc. Am. Proc. 36:237–241.

Meijer, E. M., H. W. van Verseveld, E. G. van der Beek, and A. H. Stouthamer. 1977. Energy conservation during aerobic growth in *Paracoccus denitrificans*. Arch. Microbiol. 112:25–34.

Shah, D. B., and G. A. Coulman. 1978. Kinetics of nitrification and denitrification reactions. Biotechnol. Bioeng. 20:43–72.

Smith, K. A. 1977. Soil aeration. Soil Sci. 123:284–291.

Smith, K. A. 1980. A model of the extent of anaerobic zones in aggregated soils and its potential to estimates of denitrification. J. Soil Sci. 31:263–277.

Stakman, W. P. 1974. Measuring soil moisture. *In* Drainage principles and applications: 3. Surveys and investigations. ILRI, Wageningen, The Netherlands, pp. 221–251.

Staple, W. J. 1966. Infiltration and redistribution of water in vertical columns of loam soil. Soil Sci. Soc. Am. Proc. 30:553–558.

Swart, J. G., de, and P. H. Groenevelt. 1971. Column scanning with 60 keV gamma radiation. Soil Sci. 112:419–424.

Verseveld, H. W., van, E. M. Meijer, and A. H. Stouthamer. 1977. Energy conservation during nitrate respiration in *Paracoccus denitrificans*. Arch. Microbiol. 112:17–23.

Wilhelm, E., R. Battino, and R. J. Wilcock. 1977. Low-pressure solubility of gases in liquid water. Chem. Rev. 77:219–262.

Wit, C. T., de. 1982. Simulation of living systems. *In* Simulation of plant growth and crop production. F. W. T. Penning de Vries, and H. H. van Laar (eds.). PUDOC, Wageningen, The Netherlands, pp. 3–8.

Wit, C. T., de, and H. van Keulen. 1975. Simulation of transport processes in soils. Simulation Monographs, PUDOC, Wageningen, The Netherlands, p. 100.